

BREAST CANCER RISK ASSESSMENT USING GABOR FILTER BANK AND
CURVELET TRANSFORM

ANDRES FELIPE VARGAS MOLANO

INDUSTRIAL UNIVERSITY OF SANTANDER
FACULTY OF PHYSICAL-MECHANICAL ENGINEERING
SCHOOL OF ELECTRICAL, ELECTRONIC AND TELECOMMUNICATIONS
ENGINEERING
BUCARAMANGA

2021

BREAST CANCER RISK ASSESSMENT USING GABOR FILTER BANK AND
CURVELET TRANSFORM

ANDRES FELIPE VARGAS MOLANO

A thesis to get the degree of Electronic Engineer

Director:

SAID DAVID PERTUZ ARROYO

PhD in Computer Science

INDUSTRIAL UNIVERSITY OF SANTANDER
FACULTY OF PHYSICAL-MECHANICAL ENGINEERING
SCHOOL OF ELECTRICAL, ELECTRONIC AND TELECOMUNICATIONS
ENGINEERING
BUCARAMANGA

2021

AGRADECIMIENTOS

Agradezco a Dios por la sabiduría, paciencia y fortaleza que me ha permitido superar cada uno de los obstáculos que se me presentaron. A mi familia y amigos por apoyarme y animarme a cumplir cada una de las metas propuestas. A el grupo de investigación en conectividad y procesamiento de señales (CPS) por ser parte importante en el proceso de mi crecimiento intelectual y en especial a mi director de proyecto quien me acompañó en el desarrollo de este trabajo.

Andres Felipe Vargas Molano

CONTENTS

	pag.
INTRODUCTION	10
1. DATASET.....	12
2. PROPOSED METHOD.....	13
2.1 PRE-PROCESSING	14
2.2 FEATURE EXTRACTION.....	14
2.2.1 Gabor filter banks.....	15
2.2.2 Curvelet transform.....	17
2.3 RISK SCORING.....	19
3. EXPERIMENTAL RESULTS	20
4. CONCLUSIONS	22
BIBLIOGRAPHY	23

LIST OF TABLES

pag.

Table 1. Gabor filter bank configurations.	16
Table 2. Configurations for Curvelet transform.	19
Table 3. AUC for different feature selection methods. (a) Without feature selection, (b) with stepwise feature selection and, and (c) with pre-selection of frequency bands.	20

LIST OF FIGURES

pag.

Figure 1. Flow chart of the proposed methodology. The analysis using Gabor filters and Curvelet transform only differs in the feature extraction stage.	13
Figure 2. Preprocessing: (a) Maximum circumscribed square within the breast, (b) ROI after windowing and zero padding.	14
Figure 3. Gabor filter bank configurations considered in this study. (a) distribution of frequency bands by octaves, (b) distribution of frequency bands of the same size, and (c) adjustable number of orientations.	17
Figure 4. Curvelet transform configurations: (a) Default Curvelet transform, (b) Four-bands grouping.	18

LIST OF ANNEXES

pag.

ANNEX A. DETAILED RESULTS OF AUC ESTIMATION.....	25
--	----

ABSTRACT

TITLE: BREAST CANCER RISK ASSESSMENT USING GABOR FILTER BANKS AND CURVELET TRANSFORM*

AUTHOR: ANDRES FELIPE VARGAS MOLANO**

KEY WORDS: BREAST CANCER RISK ASSESSMENT, CURVELET TRANSFORM. GABOR FILTERS, FEATURE EXTRACTION, SPATIAL FREQUENCY ANALYSIS.

DESCRIPTION: The goal of breast cancer risk assessment is to establish the risk that a healthy person has of developing breast cancer in the future. Recently, mammographic images have shown great potential for the extraction of imaging biomarkers for the construction of breast cancer risk models. The Gabor filters and the Curvelet transform decompose texture information at different scales and orientations in spatial frequency domain and they can be utilized for the analysis of mammographic texture features. This work aims at comparing the Gabor filters and Curvelet transform for the extraction of texture features for the assessment of breast cancer risk. We compared different configurations of Gabor and Curvelet filter banks by analyzing the effect of the number of bands and architecture of the filters. A feature selection process was carried out where three different scenarios were analyzed: the first one using features from all frequency bands without feature selection, the second by performing sequential forward feature selection and, the third one by performing a pre-selection of the relevant bands using a threshold of significance ($p < 0.05$) by representing each frequency band with 3 parameters (α , β and μ) of the Generalized Gaussian Distribution (GGD). Results in a pilot case-control study with 54 digital mammography images (27 cases and 27 controls) indicate that Gabor filter banks yield a superior performance than Curvelet analysis, with an AUC of 0.722 in the classification of high-risk and low-risk women.

* Bachelor Thesis

** Faculty of Physical-Mechanical Engineering. School of Electrical, Electronic and Telecommunications Engineering. Director: Said David Pertuz Arroyo, PhD in Computer Science.

RESUMEN

TÍTULO: EVALUACIÓN DE RIESGO DE CANCER DE SENO USANDO BANCOS DE FILTROS GABOR Y TRANSFORMADA CURVELET*

AUTOR: ANDRES FELIPE VARGAS MOLANO**

PALABRAS CLAVE: EVALUACIÓN DE RIESGO DE CANCER DE SENO, TRANSFORMADA CURVELET, FILTROS GABOR, EXTRACCIÓN DE CARACTERÍSTICAS, ANALISIS DE FRECUENCIA ESPACIAL.

DESCRIPCIÓN: El objetivo de la evaluación del riesgo de cáncer de seno es establecer el riesgo que tiene una persona sana de desarrollar cáncer de seno en el futuro. Recientemente, las imágenes mamográficas han mostrado un gran potencial para la extracción de biomarcadores de imagen para la construcción de modelos de riesgo de cáncer de seno. Los filtros de Gabor y la transformada Curvelet descomponen la información de textura a diferentes escalas y orientaciones en el dominio de la frecuencia espacial y se pueden utilizar para el análisis de características de textura mamográfica. Este trabajo tiene como objetivo comparar los filtros de Gabor y la transformada de Curvelet para la extracción de características de textura para la evaluación del riesgo de cáncer de seno. Comparamos diferentes configuraciones de bancos de filtros Gabor y Curvelet analizando el efecto del número de bandas y la arquitectura de los filtros. Se llevó a cabo un proceso de selección de características en el que se analizaron tres escenarios diferentes: el primero utilizando características de todas las bandas de frecuencia sin selección de características, el segundo realizando una selección secuencial de características y el tercero realizando una preselección de las bandas relevantes utilizando un umbral de significancia ($p < 0.05$) al representar cada banda de frecuencia con 3 parámetros (α , β y μ) de la Distribución Gaussiana Generalizada (GGD). Los resultados de un estudio piloto de casos y controles con 54 imágenes de mamografías digitales (27 casos y 27 controles) indican que los bancos de filtros de Gabor ofrecen un rendimiento superior al análisis de Curvelet, con un AUC de 0,722 en la clasificación de mujeres de alto y bajo riesgo.

* Trabajo de grado

** Facultad de Ingeniería Físico-mecánicas. Escuela de Ingenierías Eléctrica, Electrónica y de Telecomunicaciones. Director: Said David Pertuz Arroyo, PhD en Ciencias de la Computación.

INTRODUCTION

Breast cancer is one of the most common types of cancer worldwide. It is the second leading cause of cancer death and the leading cause of cancer death in women¹. Due to the high mortality rate, many investigations have focused their efforts on the early detection of breast cancer and on breast cancer risk assessment. In this scope, risk assessment allows health professionals to estimate the risk that a person may develop breast cancer in the future. In risk assessment, models based on mammographic breast density measurements and others based on image texture biomarkers have been developed. In recent years, the analysis of the texture of the breast parenchyma has become very important when used for risk assessment². Many computerized methods have been developed for feature extraction of medical images, some of them focused on spatial frequency analysis (SFA), such as the Gabor filters and the Curvelet transform^{3 4}.

A Gabor filter is characterized by its impulse response as it corresponds to the

¹ GHONCHEH, Mahshid; POURNAMDAR, Zahra and SALEHINIYA, Hamid. Incidence and mortality and epidemiology of breast cancer in the world. *Asian Pacific Journal of Cancer Prevention*. 2016, vol. 17, no sup3, p. 43-46.

² GASTOUNIOTI, Aimilia; CONANT, Emily F. and KONTOS, Despina. Beyond breast density: a review on the advancing role of parenchymal texture analysis in breast cancer risk assessment. *Breast cancer research*. 2016, vol. 18, no 1, p. 1-12.

³ ALVAREZ-JIMENEZ, Charlems, et al. Differentiating Cancerous and Non-cancerous Prostate Tissue Using Multi-scale Texture Analysis on MRI. In *2019 41st Annual International Conference of the IEEE Engineering in Medicine and Biology Society (EMBC)*. IEEE, 2019. p. 2695-2698.

⁴ ZAINUDIN, Muhammad Noorazlan Shah; MOHD SAID, Muzalifah and ISMAIL, Mohd Muzafar. Feature extraction on medical image using 2D Gabor filter. In *Applied Mechanics and Materials*. Trans Tech Publications Ltd, 2011. p. 2128-2132.

product of a sinusoidal function and a Gaussian function and can be interpreted as a band-pass filter in the spatial frequency domain⁵. By the adjusting the parameters of the Gabor function it is possible to modify the shape of the filter and establish the scale and orientation in the spatial frequency domain. On the other hand, the Curvelet transformation is part of the multi-scale geometric transformations. This transformation is a multi-scale pyramid with many directions and orientations⁶. The Curvelet transform has been used to differentiate cancerous and non-cancerous prostate tissue by performing a multi-scale texture analysis⁷. In this sense, the utilization of SFA transformations has shown great potential for risk assessment. Since the Gabor transform has shown great potential for breast cancer risk assessment, and the curvelet has been successful with other cancers, then it is worth comparing these two testing strategies systematically and objectively to see which one is most advantageous for breast cancer risk assessment task.

⁵ ZHENG, Yufeng. Breast cancer detection with Gabor features from digital mammograms. *algorithms*. 2010, vol.3, no 1, p. 44-62.

⁶ CANDÈS, Emmanuel, et al. Fast discrete curvelet transforms. *Multiscale Modeling & Simulation*. 2006, vol. 5, no 3, p. 861-899.

⁷ ALVAREZ-JIMENEZ. Op. Cit., p. 2695-2698.

1. DATASET

In this work, we selected a set of full field digital mammograms (FFDM) from the Breast Cancer Digital Repository (BCDR). Datasets D01 and D02 originally comprise 598 mammograms from 226 patients with biopsy-proven lesions; and set DN01 contains 200 normal mammograms from 48 women. Datasets D01 and D02 also include clinical data information, a set of intensity descriptors, a set of texture descriptors, a set of shape descriptors and lesion location, while the dataset DN01 only includes clinical data. These datasets were originally devised for diagnosis and detection tasks⁸. However, because in this work we are interested in the problem of breast cancer risk assessment, we selected a subset of images as follows: first, we selected contralateral images of the affected breast from cancer-diagnosed women. Subsequently, we selected healthy control images by matching age, laterality, view, and BI-RADS density category of the corresponding case.

The selection process of the images has two goals: on the one hand, we need to guarantee that risk assessment is performed on images without lesions. The utilization of contralateral images is a common practice for the evaluation of quantitative risk assessment methods⁹. On the second hand, we need to control the effect of known risk factors, such as patient age and breast density. Laterality and view matching was used to rule out the effect of texture orientation and overall breast shape in the analysis. As a result, we selected a set of 54 mammograms corresponding to 27 cases-control pairs. For all experiments, the reported results

⁸ MOURA, Daniel C. and LÓPEZ, Miguel A. An evaluation of image descriptors combined with clinical data for breast cancer diagnosis. *International journal of computer assisted radiology and surgery*. 2013, vol. 8, no 4, p. 561-574.

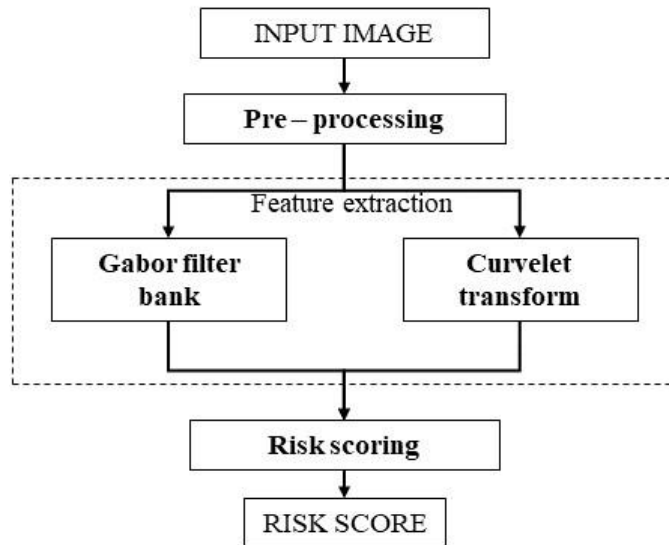
⁹ PERTUZ, Said, *et al.* Clinical evaluation of a fully-automated parenchymal analysis software for breast cancer risk assessment: A pilot study in a Finnish sample. *European journal of radiology*. 2019, vol. 121, p. 108710.

correspond to a 4-fold randomized cross-validation.

2. PROPOSED METHOD

In this work, the performance of Gabor filters and the Curvelet transform are evaluated for the task of cancer risk assessment. In general, risk assessment based on SFA can be performed in three steps: pre-processing of images, feature extraction and risk scoring. Figure 1 summarizes the methodology followed in this work to compare the performance of Gabor filters and Curvelet transform in breast cancer risk assessment. The three stages of the analysis are briefly described below.

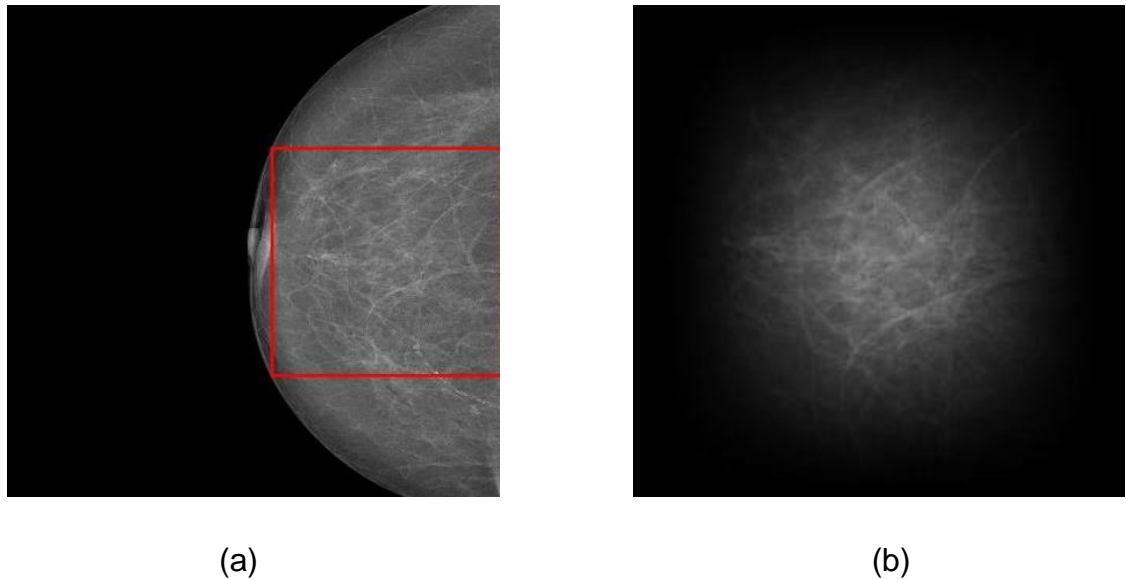
Figure 1. Flow chart of the proposed methodology. The analysis using Gabor filters and Curvelet transform only differs in the feature extraction stage.



2.1 PRE-PROCESSING

The aim of pre-processing is extracting a region of interest (ROI) from each mammogram for subsequent analysis. All mammograms were resized by a factor of 0.5 and the largest circumscribed square is found within the breast region. In order to mitigate leakage when analyzing images in the frequency domain, a Hanning window is applied to this region. In order to compensate for differences in breast size, all squared ROIs are standardized to the same number of pixels by means of zero padding. This facilitates subsequent steps in SFA by guaranteeing that spatial frequencies are analyzed properly when considering ROIs with different sizes. This process is illustrated in figure 2 In the sequel, all processing steps take place in the pre-processed ROIs.

Figure 2. Preprocessing: (a) Maximum circumscribed square within the breast, (b) ROI after windowing and zero padding.



2.2 FEATURE EXTRACTION

Studies have shown a positive association between the risk prediction generated by the quantitative analysis of features of multiscale mammographic images and the

risk that a woman will have breast cancer in the future¹⁰. For feature extraction different banks of Gabor filters and Curvelet transformation are used since they decompose the texture information in spatial frequency scales and orientations.

2.2.1 Gabor filter banks. Many features resulting from the application of Gabor filters have been studied in the literature for the classification or segmentation of textures¹¹. The convolution kernel of a Gabor filter is formed by the product between a Gaussian function and a cosine function:

$$g(x,y) = \exp\left(-\frac{\tilde{x}^2 + \gamma^2 \tilde{y}^2}{2\sigma^2}\right) \cos\left(2\pi \frac{\tilde{x}}{\lambda} + \phi\right) \quad (1)$$

with,

$$\tilde{x} = x\cos(\theta) + y\sin(\theta) \quad (2)$$

$$\tilde{y} = -x\sin(\theta) + y\cos(\theta) \quad (3)$$

where λ is the wavelength of the cosine factor, θ specifies the orientation of the Gabor filter, ϕ is the phase offset in the argument of the cosine factor, γ is the spatial aspect ratio that specifies the ellipticity of the support of the Gabor function, and σ is the standard deviation that determines the filter's bandwidth.

A two-dimensional Gabor filter behaves like a band pass filter in the spatial frequency domain. In this work, we studied three different configurations for the Gabor filter banks. In the first configuration, a distribution of frequency bands by octaves is established. In this case, the frequency bandwidth, in octaves, from frequency f_1 to

¹⁰ SUN, Wenqing, *et al.* Using multiscale texture and density features for near-term breast cancer risk analysis. *Medical physics*. 2015, vol. 42, no 6Part1, p. 2853-2862.

¹¹ GRIGORESCU, Simona E.; PETKOV, Nicolai and KRUIZINGA, Peter. Comparison of texture features based on Gabor filters. *IEEE Transactions on Image processing*. 2002, vol. 11, no 10, p. 1160-1167.

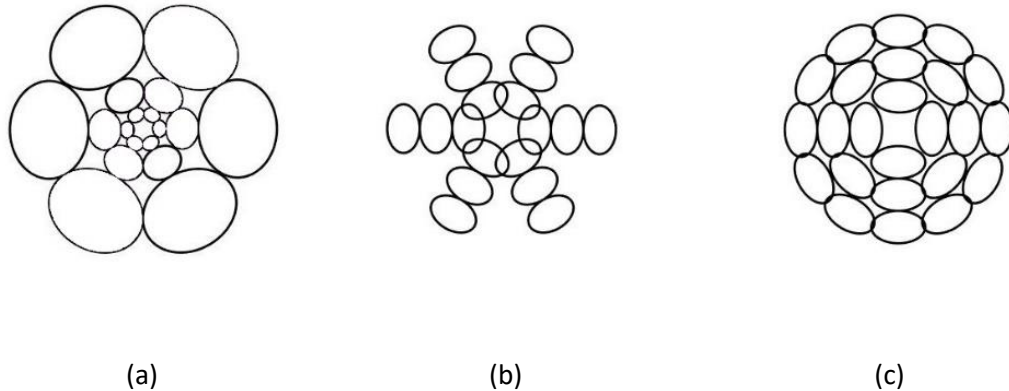
frequency f_2 is given by $\log_2(\frac{f_2}{f_1})$, where f_1 and f_2 correspond to spatial radial frequencies as shown in figure 3(a). This is the classical configuration of Gabor filter banks inspired on different experiments that have shown that the frequency bandwidth of simple cells in the visual cortex is approximately 1 octave¹². In the second configuration, a distribution of frequency bands of the same bandwidth is established at different orientations, as shown in figure 3(b). The third configuration consists of an adjusting the number of orientations of filters of the same bandwidth in each scale in order to attain full coverage of the frequency scale, as shown in figure 3(c). After applying the filter banks, the energy measurements are extracted for the image resulting from the application of each filter. For all configurations, we considered filter banks with 3, 4 and 5 scales, Table 1 shows the number of scales, orientations, and total number of features for each configuration. For the sake of brevity, we only report the best results for each configuration, which were obtained with 3 scales.

Table 1. Gabor filter bank configurations.

Configuration	Scales	Orientations	Features
Gabor 1	3	3	9
Gabor 2	3	3	9
Gabor 3	3	Adjustable	12

¹² POLLEN, Daniel A. and RONNER, Steven F. Visual cortical neurons as localized spatial frequency filters. *IEEE Transactions on Systems, Man, and Cybernetics*. 1983, no 5, p. 907-916.

Figure 3. Gabor filter bank configurations considered in this study. (a) distribution of frequency bands by octaves, (b) distribution of frequency bands of the same size, and (c) adjustable number of orientations.



2.2.2 Curvelet transform. Previous works have shown a good performance for the classification of textures based on feature extraction using the Curvelet transform. In the analysis of medical images, automated systems have been developed for tissue classification, for example, the classification of cancerous and no-cancerous prostate tissue¹³, and the Curvelet-based texture classification of tissues in medical images obtained from computed tomography (CT) scans¹⁴. The Curvelet transformation belongs to the family of multiscale geometric transformations. It is a transformation that decomposes information at different scales and orientations and is defined as the convolution between a radial window and an angular window¹⁵. Each subband of the curvelet transform represents a part of the spatial frequency

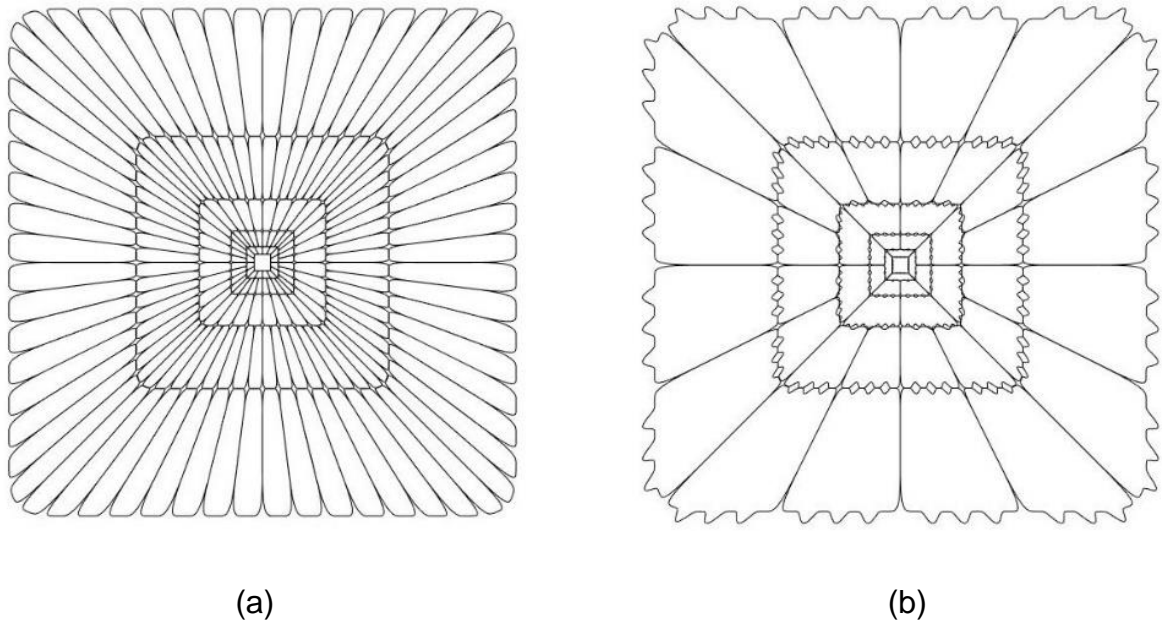
¹³ ALVAREZ-JIMENEZ. Op. Cit., p. 2695-2698.

¹⁴ DETTORI, Lucia and SEMLER, Lindsay. A comparison of wavelet, ridgelet, and curvelet-based texture classification algorithms in computed tomography. *Computers in biology and medicine*. 2007, vol. 37, no 4, p. 486-498.

¹⁵ CANDÉS, Op. Cit., p. 861-899.

domain. In this work, we studied two different configurations for the Curvelet transform. Both configurations use the wrapper-based digital implementations of the Curvelet transformation developed by Candes Emanuel *et al.*¹⁶. In the first configuration all bands are used independently as shown in figure 4(a). In the second configuration, bands are merged into groups of four bands excluding, the center as shown in figure 4(b). The aim of this configuration is to avoid redundancy in the features due to over-segmentation of the frequency bands. Table 2 shows the resulting number of features for each configuration.

Figure 4. Curvelet transform configurations: (a) Default Curvelet transform, (b) Four-bands grouping.



¹⁶ *Ibid.*, p 861-899.

Table 2. Configurations for Curvelet transform.

Configuration	Subbands per scale*					Total features
	1	2	3	4	5	
Curvelet 1	16	32	32	64	64	209
Curvelet 2	4	8	8	16	16	53

2.3 RISK SCORING

For risk scoring, the set of features extracted in previous steps are typically fed to classical machine learning algorithms¹⁷. For comparison purposes, in this work we considered two learning algorithms: a logistic regression and a support vector machine (SVM) with a linear and radial base function (RBF) kernel. For each algorithm, three different scenarios were analyzed: the first one using features from all frequency bands without feature selection, the second by performing sequential forward feature selection and, the third one by performing a pre-selection of the relevant bands using a threshold of significance ($p < 0.05$) by representing each frequency band with 3 parameters (α , β and μ) of the Generalized Gaussian Distribution (GGD). This later procedure was considered due to its good results in the classification of malignant tissue in prostate cancer using Curvelet transform¹⁸.

* Excluding de center.

¹⁷ PERTUZ, Said, *et al.* Open framework for mammography-based breast cancer risk assessment. In *2019 IEEE EMBS International Conference on Biomedical & Health Informatics (BHI)*. IEEE, 2019. P. 1-4.

¹⁸ ALVAREZ-JIMENEZ. Op. Cit., p. 2695-2698.

3. EXPERIMENTAL RESULTS

The performance was measured in terms of the area under the ROC curve (AUC), The ROC curve is plotted with true positive rate (sensitivity) against the false positive rate (1 - specificity). The results of the AUC measurement without feature selection, with stepwise feature selection, and with pre-selected frequency bands are presented in Tables 3(a), 3(b) and 3(c), In the supplementary material, we include detailed experimental results with 95 % confidence interval for AUC estimates and we also assess the statistical significance of differences in AUC using DeLong's test. The best overall results were obtained using a logistic regression classifier with the third configuration of the Gabor filter bank using feature selection with an AUC score of 0.722. In general, risk assessment with feature selection yields better performance than using either pre-selected frequency bands or without feature selection. The need for feature selection suggests that SFA can yield redundant features. As a result, feature selection is required to avoid redundancy and overfitting. With few exceptions, all configurations of the Gabor filter banks outperform Curvelet analysis.

Table 3. AUC for different feature selection methods. (a) Without feature selection, (b) with stepwise feature selection and, and (c) with pre-selection of frequency bands.

Configuration	Logistic regression	SVM - Linear	SVM - RBF
Curvelet 1	0.450	0.516	0.453
Curvelet 2	0.586	0.506	0.520
Gabor 1	0.534	0.573	0.676
Gabor 2	0.564	0.656	0.510
Gabor 3	0.503	0.624	0.479

(a)

Configuration	Logistic regression	SVM - Linear	SVM - RBF
Curvelet 1	0.501	0.409	0.595
Curvelet 2	0.719	0.554	0.498
Gabor 1	0.632	0.480	0.601
Gabor 2	0.629	0.693	0.414
Gabor 3	0.722	0.642	0.439

(b)

Configuration	Logistic regression	SVM - Linear	SVM - RBF
Curvelet 1	0.592	0.491	0.444
Curvelet 2	0.619	0.543	0.547
Gabor 1	0.556	0.562	0.671
Gabor 2	0.658	0.609	0.508
Gabor 3	0.560	0.551	0.524

(c)

* In the annex A, we include detailed experimental results with 95% confidence interval for AUC estimates and we also assess the statistical significance of differences in AUC using DeLong's test.

4. CONCLUSIONS

In this work, we studied the extraction of features based on spatial frequency analysis using Gabor filters and Curvelet transform for the task of breast cancer risk assessment from mammography images. Various configurations of Gabor filter banks and an adaptation to the Curvelet transform were developed. The highest performance was obtained with a Gabor filter bank of three scales and an adjustable number of orientations, with an AUC of 0.722 in the classification of high-risk and low-risk women in case-control study of 54 women using 4-fold cross validation. Despite the promising results of Curvelet analysis with other types of cancer, our results suggest that Gabor filter banks yield a better performance in breast cancer risk assessment. Interestingly enough, the best performance is not obtained using the classical Gabor configuration with frequency bands covering different octaves. Instead, the best performance is obtained with frequency bands of fixed bandwidth and by adjusting the number of orientations in each scale in order to cover the full frequency spectrum of the images.

BIBLIOGRAPHY

ALVAREZ-JIMENEZ, Charlems, *et al.* Differentiating Cancerous and Non-cancerous Prostate Tissue Using Multi-scale Texture Analysis on MRI. In *2019 41st Annual International Conference of the IEEE Engineering in Medicine and Biology Society (EMBC)*. IEEE, 2019. p. 2695-2698.

CANDES, Emmanuel, *et al.* Fast discrete curvelet transforms. *Multiscale Modeling & Simulation*. 2006, vol. 5, no 3, p. 861-899.

DETTORI, Lucia and SEMLER, Lindsay. A comparison of wavelet, ridgelet, and curvelet-based texture classification algorithms in computed tomography. *Computers in biology and medicine*. 2007, vol. 37, no 4, p. 486-498.

GASTOUNIOTI, Aimilia; CONANT, Emily F. and KONTOS, Despina. Beyond breast density: a review on the advancing role of parenchymal texture analysis in breast cancer risk assessment. *Breast cancer research*. 2016, vol. 18, no 1, p. 1-12.

GHONCHEH, Mahshid; POURNAMDAR, Zahra and SALEHINIYA, Hamid. Incidence and mortality and epidemiology of breast cancer in the world. *Asian Pacific Journal of Cancer Prevention*. 2016, vol. 17, no sup3, p. 43-46.

GRIGORESCU, Simona E.; PETKOV, Nicolai and KRUIZINGA, Peter. Comparison of texture features based on Gabor filters. *IEEE Transactions on Image processing*. 2002, vol. 11, no 10, p. 1160-1167.

MOURA, Daniel C. and LÓPEZ, Miguel A. An evaluation of image descriptors combined with clinical data for breast cancer diagnosis. *International journal of computer assisted radiology and surgery*. 2013, vol. 8, no 4, p. 561-574.

PERTUZ, Said, *et al.* Open framework for mammography-based breast cancer risk assessment. In *2019 IEEE EMBS International Conference on Biomedical & Health Informatics (BHI)*. IEEE, 2019. P. 1-4.

PERTUZ, Said, *et al.* Clinical evaluation of a fully-automated parenchymal analysis software for breast cancer risk assessment: A pilot study in a Finnish sample. *European journal of radiology*. 2019, vol. 121, p. 108710.

POLLEN, Daniel A. and RONNER, Steven F. Visual cortical neurons as localized spatial frequency filters. *IEEE Transactions on Systems, Man, and Cybernetics*. 1983, no 5, p. 907-916.

SUN, Wenqing, *et al.* Using multiscale texture and density features for near-term breast cancer risk analysis. *Medical physics*. 2015, vol. 42, no 6Part1, p. 2853-2862.

ZAINUDIN, Muhammad Noorazlan Shah; MOHD SAID, Muzalifah and ISMAIL, Mohd Muzafar. Feature extraction on medical image using 2D Gabor filter. In *Applied Mechanics and Materials*. Trans Tech Publications Ltd, 2011. p. 2128-2132.

ZHENG, Yufeng. Breast cancer detection with Gabor features from digital mammograms. *algorithms*. 2010, vol.3, no 1, p. 44-62.

ANNEXES

ANNEX A. DETAILED RESULTS OF AUC ESTIMATION.

The experimental results of the estimation of AUC with 95% confidence interval for the different selection strategies are presented in more detail below: without feature selection, with stepwise feature selection and with pre-selected frequency bands are presented in Tables 1, 2 and 3, respectively.

Table 1. Estimation of AUC with 95% confidence interval without feature selection.

Configuration	Logistic regression	SVM – Linear	SVM – RBF
Curvelet 1	0.450 (0.295 – 0.604)	0.516 (0.360 – 0.671)	0.453 (0.298 – 0.607)
Curvelet 2	0.586 (0.433 – 0.738)	0.506 (0.351 – 0.662)	0.520 (0.365 – 0.675)
Gabor 1	0.534 (0.379 – 0.689)	0.573 (0.420 – 0.727)	0.676 (0.533 – 0.820)
Gabor 2	0.564 (0.410 – 0.718)	0.656 (0.510 – 0.802)	0.510 (0.355 – 0.666)
Gabor 3	0.503 (0.348 -0.659)	0.624 (0.257 – 0.561)	0.479 (0.323 – 0.634)

Table 2. Estimation of AUC with 95% confidence interval with stepwise feature selection.

Configuration	Logistic regression	SVM – Linear	SVM – RBF
Curvelet 1	0.501 (0.346 – 0.657)	0.409 (0.257 – 0.561)	0.595 (0.443 – 0.747)
Curvelet 2	0.719 (0.583 – 0.856)	0.554 (0.400 – 0.708)	0.498 (0.343 – 0.653)
Gabor 1	0.632 (0.483 – 0.781)	0.480 (0.325 – 0.635)	0.601 (0.449 – 0.752)
Gabor 2	0.629 (0.480 – 0.778)	0.693 (0.552 – 0.834)	0.414 (0.261 – 0.566)
Gabor 3	0.722 (0.585 – 0.858)	0.642 (0.494 – 0.790)	0.439 (0.285 – 0.593)

Table 3. Estimation of AUC with 95% confidence interval with pre-selected frequency bands.

Configuration	Logistic regression	SVM – Linear	SVM – RBF
Curvelet 1	0.592 (0.440 – 0.744)	0.491 (0.336 – 0.646)	0.444 (0.290 – 0.599)
Curvelet 2	0.619 (0.469 – 0.769)	0.543 (0.389 -0.698)	0.547 (0.393 – 0.702)
Gabor 1	0.556 (0.401 – 0.710)	0.562 (0.408 – 0.716)	0.671 (0.527 – 0.815)
Gabor 2	0.658 (0.513 -0.804)	0.609 (0.458 – 0.760)	0.508 (0.352 – 0.663)
Gabor 3	0.560 (0.406 – 0.714)	0.551 (0.397 -0.706)	0.524 (0.369 – 0.679)

When comparing different strategies for the feature selection using the same configuration (Gabor 3) and the same learning algorithm (logistic regression), the strategy using feature selection (table 2) showed significant differences ($p < 0:05$) with respect to the other strategies.